

Slow and Fast Charge Transport Processes in PPy/NO₃ Films

Haesik Yang,^{a,*} Hochun Lee,^b Youn Tae Kim,^a and Juhyoun Kwak^{b,*z}

^aMicrosystem Team, Electronics Telecommunication Research Institute, Taejon 305-600, Korea

^bDepartment of Chemistry and School of Molecular Science, Korea Advanced Institute of Science and Technology, Taejon 305-701, Korea

The cyclic electrochemical quartz crystal microbalance (EQCM) technique and the electrochemical/electrogravimetric impedance technique have been used to reveal the ion transport mechanism of polypyrrole/nitrate (PPy/NO₃) films in the slow as well as fast charge transport processes in aqueous electrolyte solutions. The relative contributions and the relative apparent diffusion coefficients of three ions in both the slow and the fast charge transport process were obtained by assuming that the diffusion coefficients of two anions are similar, though three kinds of ions (anion and cation of an electrolyte, and another ion) take part in ion transport. It is shown that cation transport is considerable in the slow charge transport process while anion transport is dominant in the fast charge transport process.

© 2000 The Electrochemical Society. S0013-4651(99)12-116-5. All rights reserved.

Manuscript submitted December 30, 1999; revised manuscript received June 27, 2000.

Mass transport in a polypyrrole (PPy) film is rather complex. Ion transport is not permselective; some solvent transport is independent of ion transport, and ion and solvent transport are time-dependent and potential-dependent.¹⁻⁶ The change of two values (mass and charge) is obtained during the redox reaction of a film from the transient techniques such as cyclic voltammetry and electrochemical quartz crystal microbalance (EQCM),^{7,8} whereas three species (anion, cation, and solvent) are involved in mass change. Accordingly, the simple comparison between mass and charge does not give exact information on mass transport behavior.

The electrochemical impedance technique⁹⁻¹¹ has been used to obtain valuable physical values, especially an apparent diffusion coefficient in a film. The analytical equation for charge transport impedance has been proposed in case both cations and anions take part in ion transport.¹²⁻¹⁵ However, there is a limit to estimating the diffusion coefficients and the contributions of an anion and a cation by fitting impedance data to the equation because the actual charge transport process is more complex. Thus, it is necessary to obtain a more refined equation or utilize additional information such as electrogravimetric impedance¹⁶⁻²⁰ data.

Two kinds of solvent transport are possible: the solvent transport independent of ion transport and the solvent transport accompanying ion transport.⁵ The first one does not affect the electrogravimetric impedance data obtained in the steady state, whereas the effect of the second one appears in the electrogravimetric impedance data. The solvent transport accompanying ion transport makes it difficult to fit the impedance data. On the other hand, if the diffusion coefficient of an ion is equal to that of an accompanying solvent,²¹ the ion and accompanying solvent transport is regarded as the movement of a solvated ion, and three kinds of mass transport are simplified into two kinds of transport (the solvated cation transport and the solvated anion transport). It is possible to calculate the diffusion coefficient and the contribution of a solvated cation and a solvated anion by fitting both electrochemical and electrogravimetric impedance data to the known analytical equation.¹²⁻¹⁵ However, the complexity of the equation makes it difficult to fit both data simultaneously.

Generally, ion transport is coupled with electron transport. Moreover, cation transport is coupled with anion transport.¹²⁻¹⁵ If the diffusion coefficient of an electron is much larger or smaller than that of a cation and an anion, electron transport is independent of ion transport and also cation transport is independent of anion transport. Thus, the charge transport impedance is divided into the impedance for a solvated cation and the impedance for a solvated anion. Two values (the impedance data for a cation and the impedance data for an anion) can be calculated from two pieces of experimental data

(the electrochemical impedance data and the electrogravimetric impedance data). Then, the diffusion coefficient and the contribution of an anion and a cation are obtained by fitting each piece of calculated impedance data to a simple finite diffusion equation.

In many cases, only one kind of electron transport is considered in the impedance models for polymer films. In polypyrrole films, two distinct electron transports are present.²¹⁻²⁵ The presence of two semicircles in the electrochemical capacitance plot is due to the presence of two kinds of electron transport.^{21,26} We named the charge transport process related to fast electron transport the fast charge transport process, and named the process related to slow electron transport the slow charge transport process. If the fast charge transport process is much faster than the slow one, the fast charge transport is independent of the slow one. The charge transport impedance can be divided into the impedance for the fast charge transport impedance and the impedance for the slow one. Thus, the diffusion coefficient and contribution of a solvated anion and a solvated cation in each charge transport process can be calculated separately.

If the ion transport behavior in the fast charge transport process is different from that in the slow one, the overall ion transport behavior during the redox reaction of a film is time-dependent and is not ion-specific. Thus, it is important to know whether the slow charge transport process is present and also to reveal exactly the ion transport behavior in the slow charge transport process. In our previous report, anion transport is considerable in the slow charge transport process of polypyrrole/poly(styrenesulfonate) films while cation transport is dominant in the fast charge transport process.²¹

In polypyrrole/nitrate (PPy/NO₃) films, anion transport is dominant in the fast charge transport process.⁶ However, the ion transport behavior of PPy/NO₃ films in the slow charge transport process is not elucidated yet. It is known that OH⁻ transport besides anion transport is considerable during the redox reaction of PPy/NO₃ films.^{6,27,28} Thus, three kinds of ions (cation and anion of an electrolyte, and OH⁻) seem to be possible in ion transport. In this study, the ion transport behavior of PPy/NO₃ films has been investigated from the cyclic EQCM experiments and the electrochemical/electrogravimetric impedance experiments. We are able to obtain approximately the relative contributions and relative apparent diffusion coefficients of three ions in the slow as well as the fast charge transport process by assuming that the diffusion coefficient of electrolytic anion is similar to that of OH⁻.

Experimental

Chemicals, electrochemistry, and mass sensitivity.—Pyrrole, CsNO₃, Ca(NO₃)₂, and LiNO₃ were purchased from Aldrich and used as received. Doubly distilled water was used for the preparation of all solutions. An electrochemical cell and electrodes used in this study were the same as those reported previously.⁵ All potentials are

* Electrochemical Society Active Member.

^z E-mail: jhkak@kaist.ac.kr

4. The diffusion coefficient of an accompanying solvent is similar to an ion

5. The diffusion coefficients of two anions are similar.

The equivalent circuit for electrode/polymer film/electrolyte systems is shown in Fig. 2a. Z' is the charge transport impedance in polymer films. In the beginning of impedance studies for polymer films, Z' was represented as the equivalent circuit Fig. 3a (Z_D) by Ho *et al.*³⁷ and by Glarum *et al.*³⁸ This circuit was originally developed to describe a finite diffusion process of redox active species in a solution containing concentrated supporting electrolyte. Accordingly, the circuit does not represent well the charge transport impedance when ion transport and electron transport are coupled.

Albery *et al.*¹⁰ considered the film as two spatially separated phases (electron conducting phase and ion conducting phase), and assumed that the change in electron and ion concentrations is small as compared with electron and ion concentrations inside a film. In their transmission line model, Z' is represented as the circuit of Fig. 3b and the mathematical form of Z' is given by

$$Z' = R_D \left(\rho + \frac{2\rho}{\sqrt{j\omega R_D C_D} \sinh \sqrt{j\omega R_D C_D}} + \frac{1 - 2\rho}{\sqrt{j\omega R_D C_D} \tanh \sqrt{j\omega R_D C_D}} \right) \quad [1]$$

where

$$\rho = \frac{R_{De} R_{Di}}{(R_{De} + R_{Di})^2} \quad [2]$$

R_D (the charge transport resistance in a film) is the sum of R_{De} (the electronic resistance in a film) and R_{Di} (the ionic resistance in a film), C_D is the redox capacitance in a film, j is $\sqrt{-1}$, and ω is an angular frequency. If R_{De} and R_{Di} are very unequal and then ρ approaches 0, Z' is simplified as follows

$$Z' = R_D \frac{\coth \sqrt{j\omega R_D C_D}}{\sqrt{j\omega R_D C_D}} \quad [3]$$

where R_D is approximately equal to R_{De} or R_{Di} . When electron transport is much slower than ion transport, R_D is equal to R_{De} (Fig. 3c). In contrast, when ion transport is much slower than electron transport, R_D is equal to R_{Di} (Fig. 3d). Vorotyntsev *et al.*³⁹ and Mathias *et al.*^{40,41} took into account nonequilibrium charge transfer across the electrode/polymer film interface and the polymer film/electrolyte interface and obtained a more refined analytical equation. Its frequency dependence is very similar to Eq. 1.

To obtain the charge transport impedance when an electron and two kinds of ions take part in charge transport, a new equivalent circuit using the transmission line model was introduced by Albery

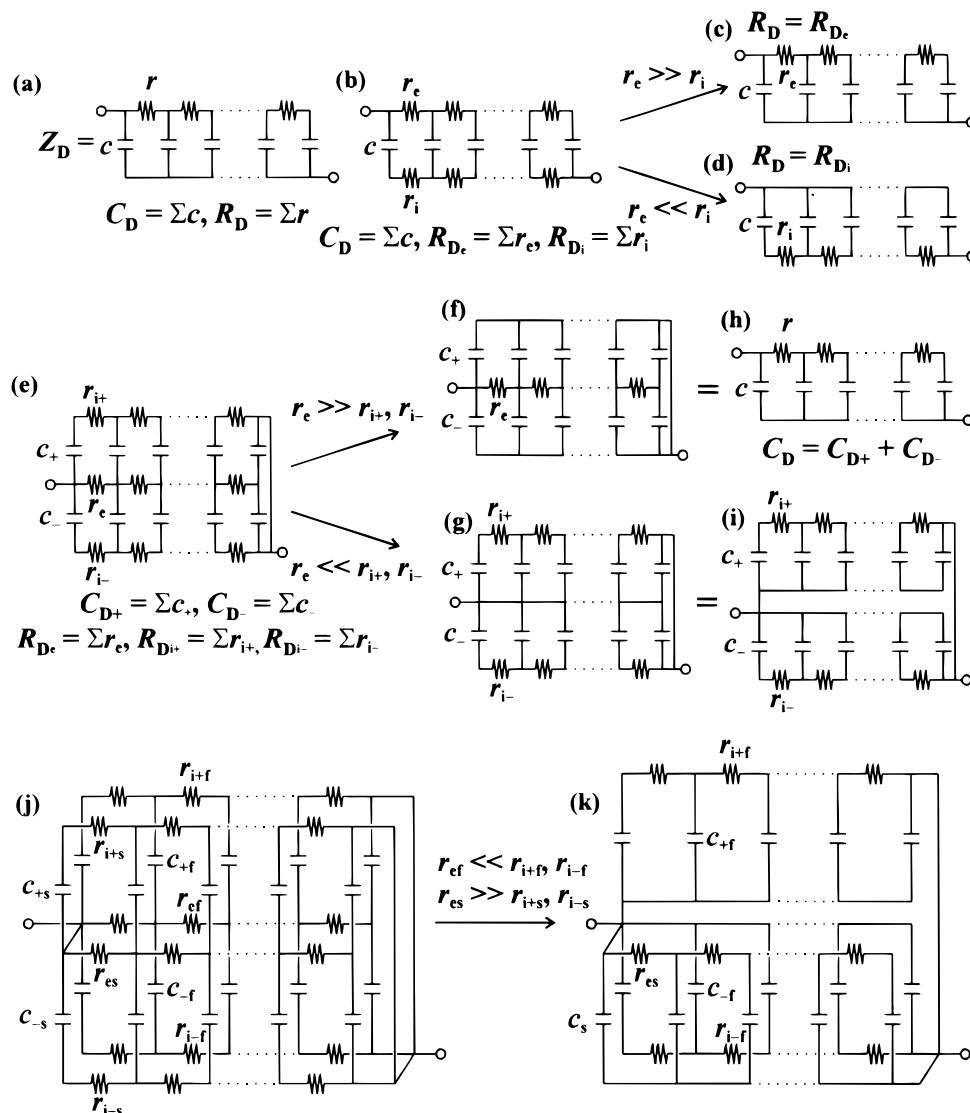


Figure 3. (a) Finite diffusion impedance of redox active species in a solution containing concentrated supporting electrolyte. (b) Finite diffusion impedance in a polymer film in the case that electron transport and ion transport are coupled; R_D , the charge transport resistance in a film ($R_D = R_{De} + R_{Di}$); R_{De} , the electronic resistance in a film; R_{Di} , the ionic resistance in a film; C_D , the redox capacitance in a film; (c) impedance when electron transport is much slower than ion transport ($R_D = R_{De}$) and (d) impedance when ion transport is much slower than electron transport ($R_D = R_{Di}$); (e) finite diffusion impedance in a polymer film in the case that both cation transport and anion transport are present; (f, h) impedance when electron transport is much slower than ion transport and (g, i) impedance when ion transport is much slower than electron transport; (j) finite diffusion impedance in the case that two kinds of electron transport are present; (k) impedance when electron transport is much faster than ion transport in the fast charge transport process and electron transport is much slower than ion transport in the slow charge transport process.

*et al.*¹³⁻¹⁵ Recently, Láng *et al.*¹² obtained an approximate analytical solution for this complex case, which was based on Vorotyntsev's approach.³⁹ However, it is not easy to use the equation in fitting the impedance data because of its complexity. If Albery's approach is used and if electron resistance is independent of the type of ion, the equivalent circuit can be represented by Fig. 3e. Moreover, if electron transport is much slower than ion transport, the equivalent circuit is represented by Fig. 3f. Finally, the circuit becomes the same as a simple Z_D (Fig. 3h). In contrast, if electron transport is much faster than ion transport, the circuit is transformed into Fig. 3g. The circuit is the same as the parallel connection of two Z_D (Fig. 3i).

It has been shown that two semicircles are present in the electrochemical capacitance plot for PPy films.²¹⁻²⁵ The presence of two separated semicircles cannot be explained just by two kinds of ion transport because the RC time for the semicircle in the high frequency region is 10^4 times smaller than that in the slow frequency region.²¹ The presence of two semicircles is due to different kinds of electron transport.^{21,26} It is known that ion transport is much slower than electron transport in the fast charge transport process of PPy films.²¹ Finally, it was concluded that ion transport is much faster than electron transport in the slow charge transport process whereas electron transport in the slow charge transport process is much slower than ion transport. Considering that the RC time for the fast charge transport process is 10^4 times smaller than that for the slow one, the slow charge transport process can be assumed to be independent of the fast charge transport process. Thus, the equivalent circuit is represented as the parallel connection of the fast charge transport impedance (Z_f) and the slow charge transport impedance (Z_s) (Fig. 2c). If each charge transport process consists of two kinds of ion transport, Z' is represented by Fig. 3j. The circuit is simplified into the parallel connection of three Z_D (Fig. 3k), because ion transport is much faster than electron transport in the slow charge transport process whereas electron transport in the slow charge transport process is much slower than ion transport.

In the same way, Z' is represented by Fig. 2d when three kinds of ions take part in charge transport. Z_f is composed of Z_{D+f} , Z_{D-1f} , and Z_{D-2f} ($1/Z_f = 1/Z_{D+f} + 1/Z_{D-1f} + 1/Z_{D-2f}$), and Z_s consists of only Z_{D_s} . The subscripts "+" and "-" represent cations and anions, respectively, and 1 and 2 represent two different anions. Though the slow charge transport process is kinetically limited by electron transport, electron transport occurs simultaneously with ion transport. Moreover, three kinds of ion transport are also possible in the slow charge transport process. Thus, Z_s can be divided into Z_{D+s} , Z_{D-1s} , and Z_{D-2s} connected parallel ($1/Z_s = 1/Z_{D+s} + 1/Z_{D-1s} + 1/Z_{D-2s}$), where $(R_{D+s}C_{D+s}) = (R_{D-1s}C_{D-1s}) = (R_{D-2s}C_{D-2s}) = (R_{D_s}C_{D_s})$, $C_{D+s} + C_{D-1s} + C_{D-2s} = C_{D_s}$, and $(1/R_{D+s} + 1/R_{D-1s} + 1/R_{D-2s}) = 1/R_{D_s}$. Figure 2e is transformed into Fig. 2f. Assuming that $R_{D-1f}C_{D-1f}$ is equal to $R_{D-2f}C_{D-2f}$, and Z_{D-1f} , Z_{D-2f} can be transformed into Z_{D-f} ($1/Z_{D-1f} + 1/Z_{D-2f} = 1/Z_{D-f}$), where $C_{D-1f} + C_{D-2f} = C_{D-f}$ and $1/R_{D-1f} + 1/R_{D-2f} = 1/R_{D-f}$. In the slow charge transport process, Z_{D-1s} and Z_{D-2s} can also be transformed into Z_{D-s} ($1/Z_{D-1s} + 1/Z_{D-2s} = 1/Z_{D-s}$) because $R_{D-1s}C_{D-1s}$ is originally the same as $R_{D-2s}C_{D-2s}$. This means that, when the diffusion coefficient of an electron is much larger or smaller than that of a cation and an anion, the impedance for a cation and the impedance for an anion can be treated independently. Finally, the approximate equivalent circuit for Z' is represented by Fig. 2g.

When one cation and two anions take part in ion transport, the relation between mass change (ΔM) and charge change (ΔQ)^{5,21} is as follows

$$\Delta M = -\frac{W'_+}{z_+F} \Delta Q_+ - \frac{W'_{-1}}{z_{-1}F} \Delta Q_{-1} - \frac{W'_{-2}}{z_{-2}F} \Delta Q_{-2} \quad [4]$$

where

$$W' = W + YW_s \quad [5]$$

In the above equations, W' is the molar mass of an ion and accompanying solvents (the apparent molar mass of an ion), z is the elec-

tric charge of an ion, F is the faradaic constant, W is the molar mass of an ion, Y is the number of accompanying solvents per ion, and W_s is the molar mass of a solvent.

If the charge transfer resistance (R_{ct}) and the double layer capacitance (C_d) are negligible, the equivalent circuit of Fig. 2a is simplified into the circuit in which Z' and the solution resistance (R_s) are connected serially (Fig. 2b). Actually, R_{ct} in many PPy films is small, and C_d is very small as compared with C_D . It was shown that, when only one kind of ion takes part in ion transport, the $(\Delta Q/\Delta E)$ data can be compared with the $(\Delta M/\Delta E)$ data without consideration of R_s .^{5,6} But, when more than two kinds of ion transport take place, the influence of R_s on the $(\Delta Q/\Delta E)$ and $(\Delta M/\Delta E)$ data must be excluded.^{20,21} When C_d is negligible, the charge change due to faradaic process (ΔQ^f) is equal to ΔQ and the mass change due to faradaic process (ΔM^f) is equal to ΔM . As shown in Fig. 2b, the ratio of the faradaic potential (ΔE^f) to the applied potential (ΔE) is equal to $(Z - R_s)/Z$, where Z is $(\Delta E/\Delta I)$. Thus, $(\Delta Q^f/\Delta E^f)$ and $(\Delta M^f/\Delta E^f)$ are represented as follows

$$\left(\frac{\Delta Q^f}{\Delta E^f}\right) = \left(\frac{\Delta Q}{\Delta E}\right) \left(\frac{\Delta E}{\Delta E^f}\right) = \left(\frac{\Delta Q}{\Delta E}\right) \left(\frac{Z}{Z - R_s}\right) \quad [6]$$

$$\left(\frac{\Delta M^f}{\Delta E^f}\right) = \left(\frac{\Delta M}{\Delta E}\right) \left(\frac{Z}{Z - R_s}\right) \quad [7]$$

The faradaic electrochemical capacitance of a cation ($\Delta Q_+^f/\Delta E^f$) and the faradaic electrochemical capacitance of two anions ($\Delta Q_{-1}^f/\Delta E^f$ and $\Delta Q_{-2}^f/\Delta E^f$) have relations with $(\Delta Q^f/\Delta E^f)$ and $(\Delta M^f/\Delta E^f)$ as follows

$$\left(\frac{\Delta Q^f}{\Delta E^f}\right) = \left(\frac{\Delta Q_+^f}{\Delta E^f}\right) + \left(\frac{\Delta Q_{-1}^f}{\Delta E^f}\right) + \left(\frac{\Delta Q_{-2}^f}{\Delta E^f}\right) \quad [8]$$

$$\begin{aligned} \left(\frac{\Delta M^f}{\Delta E^f}\right) &= \left(\frac{\Delta M_+^f}{\Delta E^f}\right) + \left(\frac{\Delta M_{-1}^f}{\Delta E^f}\right) + \left(\frac{\Delta M_{-2}^f}{\Delta E^f}\right) \\ &= -\frac{W'_+}{z_+F} \left(\frac{\Delta Q_+^f}{\Delta E^f}\right) - \frac{W'_{-1}}{z_{-1}F} \left(\frac{\Delta Q_{-1}^f}{\Delta E^f}\right) - \frac{W'_{-2}}{z_{-2}F} \left(\frac{\Delta Q_{-2}^f}{\Delta E^f}\right) \end{aligned} \quad [9]$$

Similar relations were used in our previous paper when two kinds of ion transport are present.²¹ On the other hand, Gabrielli *et al.* regard the effect of solvent transport as an independent term in Eq. 16 of their paper.²⁰ As a result, they cannot separate the contributions of a cation and an anion, and they can only judge the presence of cation, anion, or solvent transport. There is a possibility that the diffusion coefficient of a solvent in a film is different from that of an ion. In our previous papers,⁵ the semicircle and all capacitance data in the normalized electrochemical capacitance plot coincide well with the semicircle and all corresponding data in the electrogravimetric capacitance plot even though the number of accompanying waters per cation or anion is considerable. If the diffusion coefficient of a solvent were even two times larger or smaller than that of an ion, the two semicircles and both sets of two corresponding data would not coincide well. Thus, it was assumed that the diffusion coefficient of an accompanying solvent is equal to that of an ion. There is also a possibility that the number of accompanying waters per ion varies with the frequency. In this case, W'_+ , W'_{-1} , and W'_{-2} are not constants. In Fig. 6 of our previous report,⁵ the electrogravimetric capacitance plot coincides well with the normalized electrochemical capacitance plot in all frequency ranges even though the numbers of accompanying waters per ion are large. It indicates that the number of accompanying waters per ion does not vary with the frequency. Thus, we regard W'_+ , W'_{-1} , and W'_{-2} as constants. However, it is impossible to obtain three unknown values ($\Delta Q_+^f/\Delta E^f$, $\Delta Q_{-1}^f/\Delta E^f$, and $\Delta Q_{-2}^f/\Delta E^f$) from two known values ($\Delta Q^f/\Delta E^f$ and $\Delta M^f/\Delta E^f$) by solving only two equations (Eq. 8 and 9). Thus, it is required to reduce one unknown value.

In Fig. 2g, the equivalent circuit is simplified if $R_{D-1f}C_{D-1f}$ is equal to $R_{D-2f}C_{D-2f}$. When $R_{D-1f}C_{D-1f}$ is equal to $R_{D-2f}C_{D-2f}$ and $R_{D-1s}C_{D-1s}$ is equal to $R_{D-2s}C_{D-2s}$, the frequency dependence of $(\Delta Q_{-1}^f/\Delta E^f)$ is equal to that of $(\Delta Q_{-2}^f/\Delta E^f)$, and the frequency dependence of $(\Delta M_{-1}^f/\Delta E^f)$ is equal to that of $(\Delta M_{-2}^f/\Delta E^f)$. In this case, $(\Delta Q_{-1}^f/\Delta E^f)$ and $(\Delta Q_{-2}^f/\Delta E^f)$ can be summed, and $(\Delta M_{-1}^f/\Delta E^f)$ and $(\Delta M_{-2}^f/\Delta E^f)$ can be summed as follows

$$\left(\frac{\Delta Q^f}{\Delta E^f}\right) = \left(\frac{\Delta Q_{-1}^f}{\Delta E^f}\right) + \left(\frac{\Delta Q_{-2}^f}{\Delta E^f}\right) \quad [10]$$

$$\left(\frac{\Delta M^f}{\Delta E^f}\right) = \left(\frac{\Delta M_{-1}^f}{\Delta E^f}\right) + \left(\frac{\Delta M_{-2}^f}{\Delta E^f}\right) \quad [11]$$

Thus, two different anions can be regarded as one kind of anion whose charge is -1 and whose apparent molar mass is W_- . Equations 8 and 9 are simplified as follows

$$\left(\frac{\Delta Q^f}{\Delta E^f}\right) = \left(\frac{\Delta Q_+^f}{\Delta E^f}\right) + \left(\frac{\Delta Q_-^f}{\Delta E^f}\right) \quad [12]$$

$$\left(\frac{\Delta M^f}{\Delta E^f}\right) = -\frac{W_+}{z_+F} \left(\frac{\Delta Q_+^f}{\Delta E^f}\right) + \frac{W_-}{F} \left(\frac{\Delta Q_-^f}{\Delta E^f}\right) \quad [13]$$

where

$$\frac{W_-}{F} \left(\frac{\Delta Q_-^f}{\Delta E^f}\right) = -\frac{W'_{-1}}{z_{-1}F} \left(\frac{\Delta Q_{-1}^f}{\Delta E^f}\right) - \frac{W'_{-2}}{z_{-2}F} \left(\frac{\Delta Q_{-2}^f}{\Delta E^f}\right) \quad [14]$$

Because the frequency dependence of $(\Delta Q^f/\Delta E^f)$ is equal to those of $(\Delta Q_{-1}^f/\Delta E^f)$ and $(\Delta Q_{-2}^f/\Delta E^f)$, $(\Delta Q_{-1}^f/\Delta E^f)$ can be replaced by $x(\Delta Q^f/\Delta E^f)$ and $(\Delta Q_{-2}^f/\Delta E^f)$ can be replaced by $(1-x)(\Delta Q^f/\Delta E^f)$, where x is between 0 and 1. From Eq. 14, W_- is represented as follows

$$W_- = x \frac{W'_{-1}}{z_{-1}} + (1-x) \frac{W'_{-2}}{z_{-2}} \quad [15]$$

x and $1-x$ correspond to the contributions of anion 1 and 2, respectively, to anion transport. If W_- is known, the $(\Delta Q_+^f/\Delta E^f)$ and $(\Delta Q_-^f/\Delta E^f)$ data can be obtained from the $(\Delta Q^f/\Delta E^f)$ and $(\Delta M^f/\Delta E^f)$ data.

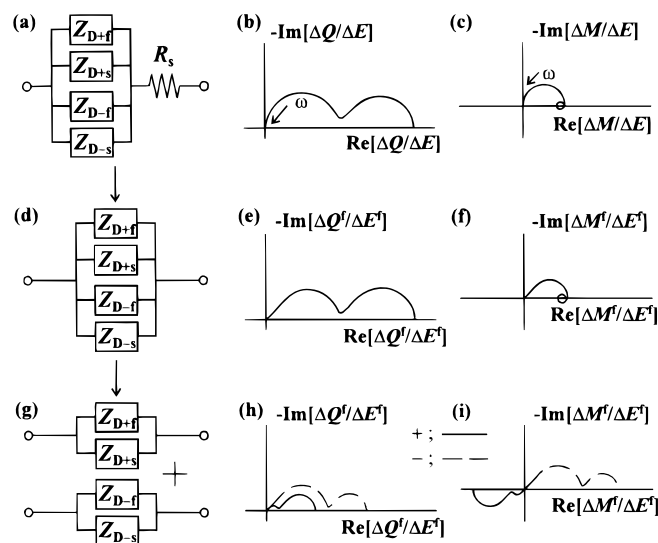


Figure 4. Flow diagram that shows how to obtain the $(\Delta Q_{-1}^f/\Delta E^f)$ and $(\Delta Q_{-2}^f/\Delta E^f)$ data from the experimental $(\Delta Q/\Delta E)$ and $(\Delta M/\Delta E)$ data.

Figure 4 is the flow diagram that shows how to obtain the $(\Delta Q_+^f/\Delta E^f)$ and $(\Delta Q_-^f/\Delta E^f)$ data from the experimental $(\Delta Q/\Delta E)$ and $(\Delta M/\Delta E)$ data. In the first step, the influence of R_s is excluded. The $(\Delta Q^f/\Delta E^f)$ and $(\Delta M^f/\Delta E^f)$ data are obtained from the $(\Delta Q/\Delta E)$ and $(\Delta M/\Delta E)$ data, respectively. And then, the $(\Delta Q_+^f/\Delta E^f)$, $(\Delta Q_-^f/\Delta E^f)$, $(\Delta M_+^f/\Delta E^f)$, and $(\Delta M_-^f/\Delta E^f)$ data are calculated from the $(\Delta Q^f/\Delta E^f)$ and $(\Delta M^f/\Delta E^f)$ data. When an anion and a cation take part in both slow and fast charge transport processes, the frequency behavior of the $(\Delta M/\Delta E)$ data (Fig. 4c) is very complex and the $(\Delta Q/\Delta E)$ plot of Fig. 4b has two semicircles. The presence of two semicircles from the $(\Delta M_+^f/\Delta E^f)$ and $(\Delta M_-^f/\Delta E^f)$ data can be easily observed in the third and the first quadrant, respectively, of the $(\Delta M^f/\Delta E^f)$ plot (Fig. 4i). In Fig. 4h, the comparison of the sizes of semicircles (C_{D+f} , C_{D+s} , C_{D-f} , and C_{D-s}) gives information on the relative contributions of anion and cation to ion transport in the fast and the slow charge transport process.

Cyclic voltammetry and capacitance plot in 0.5 M Ca(NO₃)₂.—A cyclic voltammogram and a mass change rate diagram for PPy/NO₃ films in a 0.5 M Ca(NO₃)₂ solution are shown in Fig. 5a. To compare mass change rate ($G = dM/dt$) with current (I), G is normalized by the factor $-(zF/W')$, i.e., $G_n = -(zF/W')G$. Assuming NO₃⁻-specific ion transport, G is normalized without consideration of water transport ($W' = W_{NO_3^-}$). G_n is smaller than I in an overall potential range. It was shown in the previous paper that it is due to the presence of OH⁻ transport.⁶

To investigate the ion transport behavior in the slow charge transport process, the $(\Delta Q/\Delta E)$ and $(\Delta M/\Delta E)$ data at -0.1 V are obtained in the frequency range from 2.7 Hz to 4 mHz (Fig. 6a and b). Figure 6c is a $(\Delta Q^f/\Delta E^f)$ plot, and Fig. 6d is a $(\Delta M^f/\Delta E^f)$ plot. The $(\Delta Q^f/\Delta E^f)$ data are the partial part of two semicircles. The semicircle in the higher frequency region is related to the fast charge transport process, whereas the semicircle in the lower frequency region is related to the slow charge transport process. It seems that the $(\Delta M^f/\Delta E^f)$ plot (Fig. 6d) is similar to the behavior when anion transport is much faster than cation transport.²¹ The $(\Delta M^f/\Delta E^f)$ data appear across the first and the fourth quadrant. If ion transport were anion-specific, the $(\Delta M^f/\Delta E^f)$ data would appear in the first quadrant only. It is evident that the ion transport behavior in the slow charge transport process is quite different from that in the fast one and that cation transport is considerable. Consequently, it is evident that three kinds of ion (Ca²⁺, NO₃⁻, and OH⁻) take part in ion transport.

It is shown in the previous section that the charge transport impedance is represented by Fig. 2f when two kinds of anion and one kind of cation take part in ion transport and when the redox reaction consists of the slow and the fast charge transport processes. The diffusion coefficient of an ion is inversely proportional to $R_D C_D$.²¹ If the diffusion coefficient of NO₃⁻ is equal to that of OH⁻ ($R_{D-1f}C_{D-1f} = R_{D-2f}C_{D-2f}$), the equivalent circuit for Z' can be represented by Fig. 2g. In Fig. 5 of a previous paper,⁶ the semicircle of the normalized $(\Delta Q/\Delta E)$ plot was adjusted to that of the $(\Delta M/\Delta E)$ plot, and every two sets of data of the two semicircles coincides well. If the

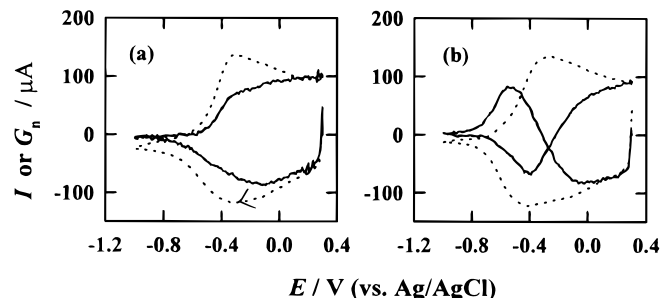


Figure 5. Cyclic voltammograms (I vs. E , ...) and normalized mass change rate diagrams (G_n vs. E , —) (scan rate = 10 mV s⁻¹, film thickness = 1.0 μm) for PPy/NO₃ films in (a) 0.5 M Ca(NO₃)₂ and (b) 1.0 M CsNO₃ ($W' = W_{NO_3^-} = 62.0$).

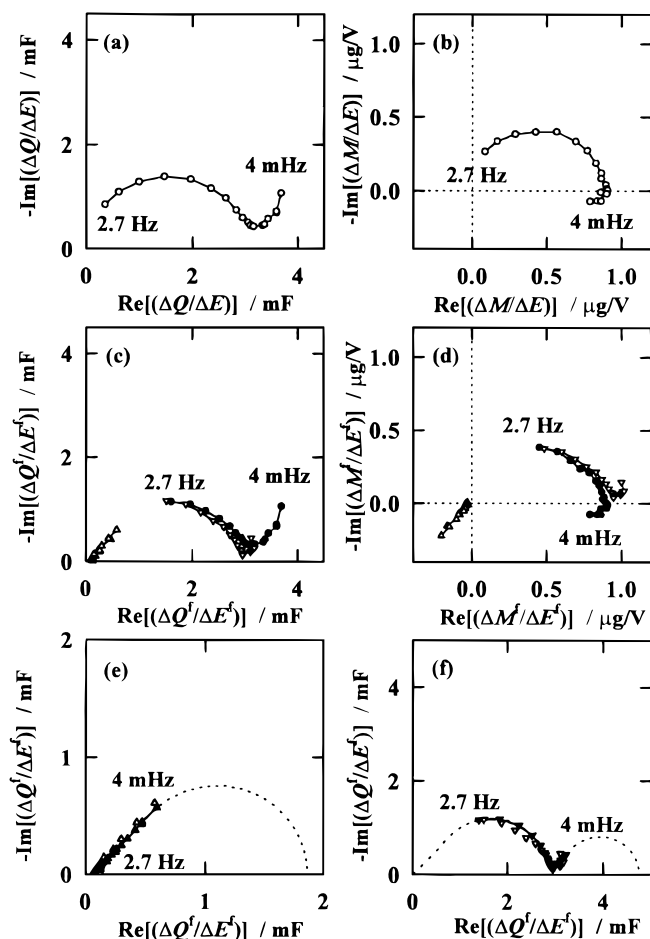


Figure 6. (a) Electrochemical capacitance ($\Delta Q/\Delta E$) plot, electrogravimetric ($\Delta M/\Delta E$) plot, (c, e, f) faradaic electrochemical capacitance ($\Delta Q^f/\Delta E^f$) plots, and (d) faradaic electrogravimetric capacitance ($\Delta M^f/\Delta E^f$) plots at $E = -0.1$ V for PPY/ NO_3 films (film thickness = $0.5 \mu\text{m}$) in $0.5 \text{ M Ca}(\text{NO}_3)_2$ ($W'_+ = 70$ and $W'_- = 31$); ($\Delta Q^f/\Delta E^f$) and ($\Delta M^f/\Delta E^f$) (\circ), ($\Delta Q^f/\Delta E^f$) and ($\Delta M^f/\Delta E^f$) (\bullet), ($\Delta Q^f_+/ \Delta E^f_+$) and ($\Delta M^f_+/\Delta E^f_+$) (\triangle), ($\Delta Q^f_+/ \Delta E^f_+$) and ($\Delta M^f_+/\Delta E^f_+$) (∇), simulated ($\Delta Q^f_+/ \Delta E^f_+$) (\blacktriangle), and simulated ($\Delta Q^f_+/ \Delta E^f_+$) (\blacktriangledown).

diffusion coefficient of NO_3^- were quite different from that of OH^- , the data would not coincide well. It indicates that the diffusion coefficient of NO_3^- is similar to that of OH^- . Thus, the faradaic electrochemical capacitance of a cation ($\Delta Q^f_+/\Delta E^f_+$) and the faradaic electrochemical capacitance of anions ($\Delta Q^f_-/\Delta E^f_-$) can be obtained by use of Eq. 12 and 13. However, W'_+ and W'_- must be known. W'_- can be calculated by adjusting the normalized $-(W'_-/zF)(\Delta Q/\Delta E)$ plot to the ($\Delta M/\Delta E$) plot in the frequency region where the fast charge transport process is dominant, if only OH^- and NO_3^- transport take place in the fast charge transport process. In Fig. 5 of our previous paper,⁶ W'_- obtained at -0.1 V in a $0.5 \text{ M Ca}(\text{NO}_3)_2$ solution is 31. In this case, the film thickness is $1 \mu\text{m}$ where the fast charge trans-

port process is dominant from 2.72-0.04 Hz. It seems that 31 is similar to the value when the slow charge transport process is not present. Thus, W'_- is regarded as 31. Though the exact value of W'_+ for Ca^{2+} is not known, it seems that W'_+ is much larger than $W_{\text{Ca}^{2+}}$ because of accompanying waters. By considering the previous result that the number of accompanying waters per Mg^{2+} is 2.2, W'_+ for Ca^{2+} is regarded as 70 or 100. The calculated ($\Delta Q^f_+/\Delta E^f_+$) and ($\Delta Q^f_-/\Delta E^f_-$) data of Fig. 6c, e, and f were obtained by use of W'_+ (70). The ($\Delta Q^f_+/\Delta E^f_+$) plot (Fig. 6e) consists of one semicircle, whereas the ($\Delta Q^f_-/\Delta E^f_-$) plot (Fig. 6f) consists of two semicircles. In case of W'_+ (100), the ($\Delta Q^f_+/\Delta E^f_+$) and ($\Delta Q^f_-/\Delta E^f_-$) plots also show similar behavior. The semicircle of the ($\Delta Q^f_+/\Delta E^f_+$) plot has a little shift from the origin. It seems to be due to a little difference between the used W'_- value and the real value. The difference does not give significant error to the ($\Delta Q^f_+/\Delta E^f_+$) and ($\Delta Q^f_-/\Delta E^f_-$) data. However, it is difficult to fit the ($\Delta Q^f_+/\Delta E^f_+$) data to the circuit consisting of only Z_{D+s} . Thus, the ($\Delta Q^f_+/\Delta E^f_+$) data must be fitted to the circuit in which Z_{D+s} and C_{D+f} are connected in parallel. Actually, the equivalent circuit of Fig. 2h is used as Z' in this experiment. The values of fitted parameters are shown in Table I. It is evident that cation transport is considerable in the slow charge transport process. But, it is difficult to verify whether anion transport is present in the slow charge transport process even though the C_{D-s} value is quite large because there are several error sources, such as the use of the wrong W'_- and W'_+ values. It is interesting to note that $R_{D-f}C_{D-f}$ is approximately 10^3 or 10^4 times smaller than $R_{D+s}C_{D+s}$ (Table I), indicating that the diffusion coefficient of anions in the fast charge transport process is at least 10^3 times larger than the apparent diffusion coefficient of Ca^{2+} in the slow charge transport process. Consequently, in PPY/ NO_3 films, anion transport is dominant in the fast charge transport process, whereas cation transport is considerable in the slow charge transport process.

It was shown that cation transport is negligible in the cyclic EQCM experiment.⁶ However, we can know from the impedance experiments that cation transport is considerable in the slow charge transport process. That is because, in the cyclic EQCM experiment, the charge transport of relatively thick films is governed by the fast charge transport process.

Cyclic voltammetry in 1 M CsNO₃ and capacitance plot in thin films.—A cyclic voltammogram and mass change rate diagram in a 1.0 M CsNO_3 solution are also shown in Fig. 5b. G is also normalized by assuming NO_3^- -specific ion transport ($W' = W_{\text{NO}_3^-}$). At a more positive potential, G_n shows similar behavior with that in a solution containing a divalent Ca^{2+} (Fig. 5a). However, in a more negative potential region, G_n is positive during the cathodic scan and it is negative during the anodic scan. It means that the mass increases during the cathodic scan and that it decreases during the anodic scan. It indicates that Cs^+ transport is considerable in the cyclic EQCM experiment and that Cs^+ transport increases as the applied potential decreases.

The frequency dependence of a semicircle in the ($\Delta Q/\Delta E$) plot is related to the diffusion coefficient of an ion. The diffusion coefficient is proportional to $l^2/R_D C_D$, where l is the film thickness.²¹ As l decreases, $R_D C_D$ decreases and the ($\Delta Q/\Delta E$) data in the given frequency range are located more to the right side of an electrochemical semicircle. If two experimental conditions are identical except

Table I. Values of the parameters obtained by fitting the faradaic electrochemical capacitance ($\Delta Q^f/\Delta E^f$) data of Fig. 6e and f in $0.5 \text{ M Ca}(\text{NO}_3)_2$ to the equivalent circuit of Fig. 2h.

W'_+ (g mol^{-1})	E (V)	R_s (Ω)	Cation				Anion			
			C_{D+f} (mF)	$R_{D+f}C_{D+f}$ (s)	C_{D+s} (mF)	$R_{D+s}C_{D+s}$ (s)	C_{D-f} (mF)	$R_{D-f}C_{D-f}$ (s)	C_{D-s} (mF)	$R_{D-s}C_{D-s}$ (s)
70	-0.1	41	0.05		1.8	240	2.8	1.9×10^{-1}	1.9	430
100	-0.1	41	0.04		4.2	1800	2.8	1.8×10^{-1}	5.5	2200

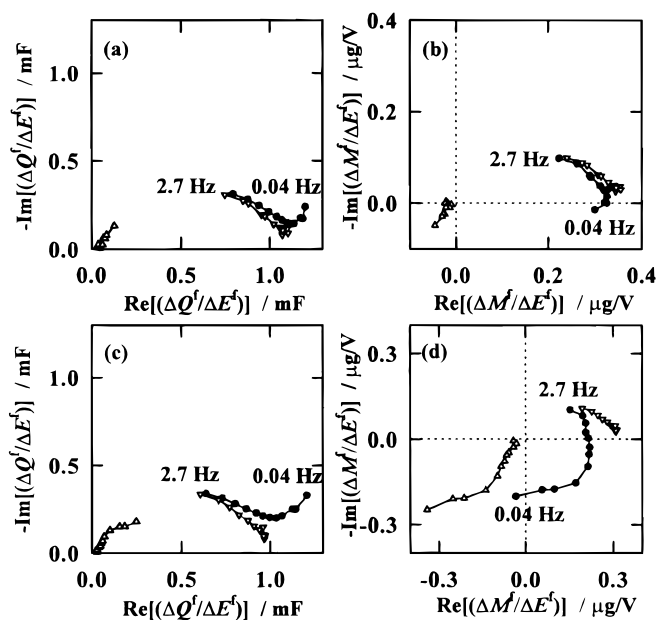


Figure 7. (a, c) Faradaic electrochemical capacitance ($\Delta Q^f/\Delta E^f$) plots and (b, d) faradaic electrogravimetric capacitance ($\Delta M^f/\Delta E^f$) plots for PPY/ NO_3 films (film thickness = 0.2 μm) at $E = -0.1$ V in (a, b) 0.5 M $\text{Ca}(\text{NO}_3)_2$ ($W_+^f = 70$ and $W_-^f = 31$) and (c, d) 1.0 M CsNO_3 ($W_+^f = C_{\text{Cs}^+} = 132.9$ and $W_-^f = 31$); ($\Delta Q^f/\Delta E^f$) and ($\Delta M^f/\Delta E^f$) (\bullet), ($\Delta Q_+^f/\Delta E^f$) (Δ), and ($\Delta Q_-^f/\Delta E^f$) and ($\Delta M_-^f/\Delta E^f$) (∇).

for the film thickness, the influence of the slow charge transport process is observed much more easily in the thinner film. Thus, the presence of anion transport in the slow charge transport process can be elucidated easily in the thinner film. Figure 7a and b show

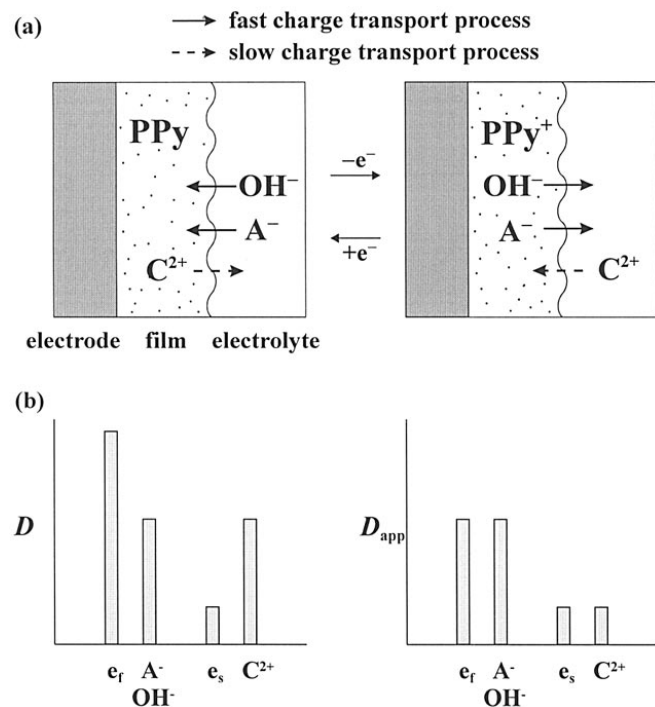


Figure 8. (a) Schematic diagrams of ion transport (A; anion, C; cation), and (b) the relative magnitude of the diffusion coefficient (D) and the apparent diffusion coefficient (D_{app}) in the fast and the slow charge transport process (e_f and e_s : electrons in the fast and the slow charge transport process, respectively) during the redox reaction of PPY/ NO_3 films in an aqueous solution containing a divalent cation.

($\Delta Q^f/\Delta E^f$) and ($\Delta M^f/\Delta E^f$) plots for 0.2 m thick PPY/ NO_3 films in a 0.5 M $\text{Ca}(\text{NO}_3)_2$ solution. It seems that both ($\Delta Q_+^f/\Delta E^f$) and ($\Delta Q_-^f/\Delta E^f$) plots consist of one semicircle. It indicates that anion transport is not large in the slow charge transport process. Figure 7c and d show ($\Delta Q^f/\Delta E^f$) and ($\Delta M^f/\Delta E^f$) plots for 0.2 μm thick PPY/ NO_3 films in a 1 M CsNO_3 solution. W_-^f and W_+^f are regarded as 31 and W_{Cs^+} , respectively, by considering that the number of accompanying waters per Cs^+ is not large.⁵ It seems that both ($\Delta Q_+^f/\Delta E^f$) and ($\Delta Q_-^f/\Delta E^f$) plots consist of one semicircle. It also shows that anion transport is not large in the slow charge transport process. It is interesting to note that the ($\Delta Q^f/\Delta E^f$) plot of Fig. 7a is similar to that of Fig. 7c, whereas the ($\Delta M^f/\Delta E^f$) plot of Fig. 7b is quite different from that of Fig. 7d. It indicates that the effect of cation transport in the slow charge transport process is much more evident in a CsNO_3 solution than a $\text{Ca}(\text{NO}_3)_2$ solution. Thus, in the cyclic EQCM experiment, cation transport is observed easily in a CsNO_3 solution (Fig. 5b), though cation transport is not observed in a $\text{Ca}(\text{NO}_3)_2$ solution (Fig. 5a).

Schematic diagram of ion transport.—It was shown that the apparent diffusion coefficient of an ion in the fast charge transport process is governed by the diffusion coefficient of an ion, whereas the apparent diffusion coefficient of an ion in the slow charge transport process is governed by the diffusion coefficient of an electron.²¹ It is shown that, in PPY/ NO_3 films, anion transport is dominant in the fast charge transport process whereas cation transport is considerable in the slow one. Figure 8a shows a schematic diagram of ion transport, and Fig. 8b shows the relative magnitude of the diffusion coefficient and the apparent diffusion coefficient in the fast and slow charge transport processes. The apparent diffusion coefficient in the fast charge transport process is related mainly to anion transport, whereas the apparent diffusion coefficient in the slow charge transport process is related mainly to electron transport.

Conclusions

The ion transport behavior in the slow as well as fast charge transport process of PPY/ NO_3 films was studied. Though three kinds of ion (OH^- , and anion and cation of electrolyte) take part in ion transport, the relative contributions and the relative apparent diffusion coefficients of the three ions was obtained approximately. It is shown that cation transport is considerable in the slow charge transport process while anion transport is dominant in the fast charge transport process. The apparent diffusion coefficient of NO_3^- and OH^- in the fast charge transport process is at least 10^3 times larger than the apparent diffusion coefficient of Ca^{2+} in the slow charge transport process. It seems that, even though three kinds of ion take part in ion transport, it is possible to obtain approximately the relative contribution and relative apparent diffusion coefficient only if two ions have similar diffusion coefficients irrespective of their sign.

Acknowledgments

This work was supported in part by the Korea Science and Engineering Foundation through the MICROS center at KAIST, Korea.

Korea Advanced Institute of Science and Technology assisted in meeting the publication costs of this article.

References

- G. Maia, R. M. Torresi, E. A. Ticianelli, and F. C. Nart, *J. Phys. Chem.*, **100**, 15910 (1996).
- R. John and G. G. Wallace, *J. Electroanal. Chem.*, **354**, 145 (1993).
- C. S. C. Boase, S. Basak, and K. Rajeshwar, *J. Phys. Chem.*, **96**, 9899 (1992).
- K. Naoi, M. Lien, and W. H. Smyrl, *J. Electrochem. Soc.*, **138**, 440 (1991).
- H. Yang and J. Kwak, *J. Phys. Chem. B*, **101**, 774 (1997).
- H. Yang and J. Kwak, *J. Phys. Chem. B*, **101**, 4656 (1997).
- D. A. Buttry and M. D. Ward, *Chem. Rev.*, **92**, 1355 (1992).
- D. A. Buttry, in *Electroanalytical Chemistry*, A. J. Bard, Editor, Vol. 17, p. 1, Marcel Dekker, New York (1991).
- P. G. Bruce, in *Polymer Electrolyte Reviews-I*, J. R. MacCallum and C. A. Vincent, Editor, Chap. 8, Elsevier, London (1987).
- W. J. Albery, C. M. Elliott, and A. R. Mount, *J. Electroanal. Chem.*, **288**, 15 (1990).
- C. Deslouis, M. M. Musiani, B. Tribollet, and M. A. Vorotyntsev, *J. Electrochem. Soc.*, **142**, 1902 (1995).
- G. Láng and G. Inzelt, *Electrochim. Acta*, **44**, 2037 (1999).
- W. J. Albery and A. R. Mount, *J. Electroanal. Chem.*, **325**, 95 (1992).

14. W. J. Albery and A. R. Mount, *J. Chem. Soc., Faraday Trans.*, **89**, 2487 (1993).
15. W. J. Albery and A. R. Mount, *J. Electroanal. Chem.*, **388**, 1 (1995).
16. S. Cordoba-Torresi, C. Gabrielli, M. Keddad, H. Takenouti, and R. Torresi, *J. Electroanal. Chem.*, **290**, 269 (1990).
17. C. Gabrielli, M. Keddad, H. Perrot, and R. Torresi, *J. Electroanal. Chem.*, **378**, 85 (1994).
18. O. Bohnke, B. Vuillemin, C. Gabrielli, M. Keddad, and H. Perrot, *Electrochim. Acta*, **40**, 2765 (1995).
19. C. Gabrielli, M. Keddad, N. Nadi, and H. Perrot, *Electrochim. Acta*, **44**, 2095 (1999).
20. C. Gabrielli, M. Keddad, H. Perrot, M. C. Pham, and R. Torresi, *Electrochim. Acta*, **44**, 4217 (1999).
21. H. Yang and J. Kwak, *J. Phys. Chem. B*, **102**, 1982 (1998).
22. T. Amemiya, K. Hashimoto, and A. Fujishima, *J. Phys. Chem.*, **97**, 4187 (1993).
23. T. Amemiya, K. Hashimoto, and A. Fujishima, *J. Phys. Chem.*, **97**, 9736 (1993).
24. X. Ren and P. G. Pickup, *J. Phys. Chem.*, **97**, 3941 (1993).
25. X. Ren and P. G. Pickup, *Electrochim. Acta*, **41**, 1877 (1996).
26. T. Amemiya, K. Hashimoto, and A. Fujishima, *J. Electroanal. Chem.*, **377**, 143 (1994).
27. Y. Li and R. Qian, *Synth. Met.*, **28**, C127 (1989).
28. Y. Li and R. Qian, *J. Electroanal. Chem.*, **362**, 267 (1993).
29. S. Bourkane, C. Gabrielli, and M. Keddad, *Electrochim. Acta*, **34**, 1081 (1989).
30. E. O. Brigham, *The Fast Fourier Transform and Its Applications*, Prentice-Hall, New York (1988).
31. H.-J. Huang, P. He, and L. R. Faulkner, *Anal. Chem.*, **58**, 2889 (1986).
32. G. S. Popkurov and R. N. Schindler, *Rev. Sci. Instrum.*, **63**, 5366 (1992).
33. G. S. Popkurov and R. N. Schindler, *Rev. Sci. Instrum.*, **64**, 3111 (1993).
34. G. S. Popkurov and R. N. Schindler, *Electrochim. Acta*, **39**, 2025 (1994).
35. G. Mészáros and L. Mészáros, *Electrochim. Acta*, **40**, 2675 (1995).
36. G. S. Popkurov and R. N. Schindler, *Electrochim. Acta*, **38**, 861 (1993).
37. C. Ho, I. D. Raistrick, and R. A. Huggins, *J. Electrochem. Soc.*, **127**, 343 (1980).
38. S. H. Glarum and J. H. Marshall, *J. Electrochem. Soc.*, **127**, 1467 (1980).
39. M. A. Vorotyntsev, L. I. Daikhin, and M. D. Levi, *J. Electroanal. Chem.*, **364**, 37 (1994).
40. M. F. Mathias and O. Haas, *J. Phys. Chem.*, **96**, 3174 (1992).
41. M. F. Mathias and O. Haas, *J. Phys. Chem.*, **97**, 9217 (1993).